FN1, a reliable prognostic biomarker for thyroid cancer, is associated with tumor immunity and an unfavorable prognosis

HUILI PAN[1*], ZHIYAN LUO[2*], FENG LIN[3*], JING ZHANG[4], TING XIONG[5], YURONG HONG[2], BOHAO SUN[4] and YAN YANG[1]

[1]Department of Nursing, Second Affiliated Hospital, School of Medicine, Zhejiang University, Hangzhou, Zhejiang 310009, P.R. China; [2]Department of Ultrasound in Medicine, Second Affiliated Hospital, School of Medicine, Zhejiang University, Hangzhou, Zhejiang 310009, P.R. China; [3]Department of Neurology, Taizhou Hospital of Zhejiang Province Affiliated to Wenzhou Medical University, Taizhou, Zhejiang 317000, P.R. China; [4]Department of Pathology, Second Affiliated Hospital, School of Medicine, Zhejiang University, Hangzhou, Zhejiang 310009, P.R. China; [5]Zhejiang Provincial Key Laboratory of Medical Genetics, School of Laboratory Medicine and Life Sciences, Wenzhou Medical University, Wenzhou, Zhejiang 325035, P.R. China

Received March 5, 2024; Accepted July 10, 2024

DOI: 10.3892/ol.2024.14643

Abstract. Thyroid cancer (THCA) is a malignant tumor that affects the endocrine system. At present, an effective treatment for THCA remains elusive, particularly for medullary carcinoma and undifferentiated carcinoma, due to the lack of suitable medications and prognostic markers. Patient RNA-sequencing and clinical data were obtained from The Cancer Genome Atlas and Genotype-Tissue Expression databases. Protein-protein interaction analyses were performed for differentially expressed genes related to THCA. Moreover, the associations between fibronectin 1 (FN1), clinical data, immune checkpoint genes and immune cell infiltration was assessed. The potential functional role of the FN1 gene was evaluated through gene set enrichment analysis. Immunohistochemistry was used to assess FN1 expression in 103 cases of THCA, comprising 32 with papillary carcinoma, 30 with follicular carcinoma, 35 with medullary carcinoma and 6 with undifferentiated carcinoma. Finally, 11 co-expression modules were constructed and the expression of five identified hub genes (FN1, mucin-1, keratin 19, intracellular adhesion molecule 1 and neural cell adhesion molecule) were evaluated. The results demonstrated that higher FN1 gene expression levels were strongly associated with a higher pathologic stage and tumor stage, and were significantly associated with immune cell infiltration in THCA. Significant increases in FN1 protein expression levels were noted among patients diagnosed with four types of THCA, comprising papillary carcinoma, follicular carcinoma, medullary carcinoma and undifferentiated carcinoma. Patients diagnosed with medullary carcinoma and undifferentiated carcinoma, and with low FN1 expression levels, exhibited a significant survival advantage compared with those with high FN1 expression levels. In conclusion, the present study identified five hub genes involved in the onset and progression of THCA. Furthermore, FN1 could serve as a candidate biomarker and a therapeutic target for THCA and may be a key gene mediating THCA immune infiltration.

Correspondence to: Dr Yan Yang, Department of Nursing, Second Affiliated Hospital, School of Medicine, Zhejiang University, 88 Jiefang Road, Hangzhou, Zhejiang 310009, P.R. China
E-mail: 2201031@zju.edu.cn

Dr Bohao Sun, Department of Pathology, Second Affiliated Hospital, School of Medicine, Zhejiang University, 88 Jiefang Road, Hangzhou, Zhejiang 310009, P.R. China
E-mail: 2521083@zju.edu.cn

*Contributed equally

Key words: fibronectin 1, thyroid cancer, hub genes, bioinformatics analysis, The Cancer Genome Atlas

Introduction

Thyroid cancer (THCA) is the most common endocrine malignancy of the head and neck globally, with a steadily increasing global incidence. It accounts for ~1% of all systemic malignant tumors (1,2). THCA comprises four pathological types: Papillary carcinoma, follicular carcinoma, undifferentiated carcinoma and medullary carcinoma (3,4). Papillary carcinoma, the most prevalent type, is characterized by low malignancy and a favorable prognosis (5). In the early stages, THCA frequently presents no noticeable symptoms or signs (6). However, in the advanced stages, hoarseness, dyspnea and compression of the sympathetic nerve can induce Horner syndrome. The etiology of THCA is not yet fully understood, but it is presently believed to result from the synergistic interaction of several carcinogenic factors, such as dietary practices, obesity and radiation exposure (7).

Most patients with THCA have a favorable outcome due to modern comprehensive treatments that include surgery, the use of radioactive iodine (RAI) thyroid ablation and thyroid stimulating hormone (TSH) suppression (8). Nevertheless, a considerable number of patients exhibit insensitivity to RAI

ablation and TSH suppression (9) and there is still a lack of standard treatment for highly aggressive and poorly differentiated tumors, which often progress to advanced tumors (10).

With the advancing comprehension of the tumor microenvironment (TME), immunotherapy has attracted increasing attention and demonstrated remarkable efficacy in combating several cancers. The programmed cell death protein 1/programmed death-ligand (PD-L)1 inhibitor pembrolizumab, known to improve the overall survival of patients with THCA, especially those with increased PD-L1 receptor expression, has been approved as a first-line treatment for THCA (11-13). Moreover, patients with THCA, particularly those with undifferentiated carcinoma, exhibit a dismal 5-year survival rate (14). Hence, there exists a pressing necessity to thoroughly investigate the intricacies of the TME and discover novel molecular targeted therapies and immunotherapies for addressing these aggressive tumors.

Several studies have reported gene mutations in THCA, with BRAF V600E being the most prevalent mutation, occurring in up to 58.5% of cases (15,16). Mutations in RAS and P53 genes are also frequently observed in THCA (17). Furthermore, in recent years, the advancement of next-generation high-throughput sequencing technologies has led to the accumulation of extensive genetic data and clinical information within several public databases, including the Cancer Genome Atlas (TCGA) (18,19). This sets the groundwork for deepening the understanding of the molecular mechanisms of cancer and the biological roles of key genes through bioinformatics techniques and experimental validation.

Fibronectin 1 (FN1) encodes a glycoprotein present in soluble dimeric form in plasma and as dimers or multimers on the cell surface and extracellular matrix (ECM). FN1 serves a key role in cell adhesion, growth, differentiation and migration, including in wound healing and embryonic development, host defense, blood clotting and metastasis (20). FN1 is deposited into the ECM of tumor cells and then forms fibronectin-fibronectin complexes, which have been reported to promote tumor angiogenesis, proliferation and metastasis (21). FN1 has also been reported to promote cell migration in esophageal squamous cell carcinoma, oral squamous cell carcinoma, nasopharyngeal carcinoma, colorectal cancer, ovarian cancer and renal cell carcinoma (22-26). Moreover, previous studies have reported that FN1 is involved in natural killer (NK) cell-produced interferon-γ mediated by the NKp46 receptor, thereby controlling tumor architecture and metastasis (27). However, the relationship between FN1 expression and clinical factors and prognosis in THCA has not been previously reported, to the best of our knowledge, and so it is necessary to validate and elucidate the role of FN1 in THCA. Therefore, the present study aimed to identify potential gene biomarkers, offering new insights into therapeutic targets for THCA.

Materials and methods

Data acquisition from the TCGA, Genotype-Tissue Expression (GTEx) and Gene Expression Omnibus (GEO) databases. Gene expression data, clinical data and survival information for THCA and normal tissues were retrieved from the Genomics Data Commons TCGA THCA and the GTEx databases (https://xenabrowser.net/datapages/). The retrieved clinical data is presented in Table SI. In total, 509 samples of THCA and 337 samples of normal thyroid tissues were obtained from the TCGA and GTEx databases. The validation cohorts, consisting of complete expression profile data (GSE33630 and GSE54958), were obtained from the GEO database (https://www.ncbi.nlm.nih.gov/gds).

Identification and analysis of differentially expressed genes (DEGs). Bioinformatics analysis was performed using RStudio software (Posit Software, PBC; version 1.4.1103) and the Bioconductor suite of packages (version 3.18; https://bioconductor.org/install/). The gene expression data was normalized and DEGs were determined using the R limma package (version 3.58.2) (https://www.bioconductor.org/packages/release/bioc/html/limma.html) (28,29). Significant DEGs were selected based on the criteria of $P<0.05$ and log fold change (FC)>1 (30,31).

Weighted gene co-expression network analysis (WGCNA). The analysis of gene co-expression networks was performed using the WGCNA R package (version 1.72.3; https://cran.r-project.org/web/packages/WGCNA/index.html) (32). The scale-free and average connectivity analyses were executed on modules with diverse power values using the PickSoftThreshold function, setting the soft threshold power to 8. Following this, the intramodular connectivity among genes displaying comparable expression profiles was calculated using the topological overlap dissimilarity measure. Finally, the dynamic hybrid cutting method was used to construct a hierarchical clustering tree and to detect co-expressed gene modules.

Construction of protein-protein interaction (PPI) network and identification of hub genes. The STRING database (http://www.string-db.org/) was used to construct a PPI network of candidate genes (33). Genes meeting the minimum confidence score of ≥0.5 for differential expression were selected to construct a comprehensive network model, which was then visualized using Cytoscape software (version 3.10; https://cytoscape.org/). Using the Cytoscape plugin cytoHubba, the top five key genes were predicted based on the network maximal clique centrality algorithm.

Functional and pathway enrichment analyses. Gene Ontology (GO) and Kyoto Encyclopedia of Genes and Genomes (KEGG) enrichment analyses were performed on the candidate hub genes of THCA using the R packages clusterProfiler (version 3.42.2; https://www.bioconductor.org/packages/release/bioc/html/clusterProfiler.html) (34). These analyses aimed to assess the biological functions and key signaling pathways associated with the identified hub genes. The GO enrichment analysis was comprehensively performed across three domains: Biological processes (BP), cellular components (CC) and molecular functions (MF) (35). Gene set enrichment analysis (GSEA) was performed using the R package GSEA (version 4.1.2; https://bioconductor.org/packages/release/bioc/html/GSEABase.html), with a significance threshold set at a false discovery rate of <0.25 and $P<0.05$.

Immunoinfiltration analysis. The analysis of immune cell infiltration was performed using the single-sample GSEA algorithm (36). A total of 28 different types of gene sets that characterize immune cells were compared and the Gene Set Variation Analysis R package (version 3.42.2; https://www.bioconductor.org/packages/release/bioc/html/GSVA.html) was used to transform sample gene expression values into enrichment fractions, thereby deriving the relative abundance of immune cells (37).

Patient and tissue samples. The study procedures were approved by the Ethics Committee of the Second Affiliated Hospital of Zhejiang University School of Medicine (Hangzhou, China) and the present study adhered to the ethical principles outlined in The Declaration of Helsinki. The inclusion criteria of the study consisted of the following: i) Presence of a primary thyroid tumor; ii) histopathological diagnosis of THCA; and iii) availability of complete clinical records. Conversely, the exclusion criteria were as follows: i) Presence of autoimmune disorders or infectious diseases; ii) presence of other malignant tumors; and iii) history of prior immunosuppressive treatments. Patient follow-up started at August 2020 and continued until November 2023, where the conclusive determination of survival or death marked the endpoint for overall survival. A total of 103 patients with THCA, specifically 32 with papillary carcinoma, 30 with follicular carcinoma, 35 with medullary carcinoma and 6 with undifferentiated carcinoma, were selected for the present study. These patients had previously undergone surgical resection at the Second Affiliated Hospital, School of Medicine, Zhejiang University. The medullary and undifferentiated carcinoma samples of THCA and their corresponding medical information were collected. Furthermore, 103 THCA tissues and their corresponding adjacent paracancerous tissues were obtained from the Department of Pathology, Second Affiliated Hospital, School of Medicine, Zhejiang University. These tissues were the same as those collected from the 103 patients enrolled in the present study.

Reverse transcription (RT)-quantitative (q)PCR. Total RNA was isolated utilizing the TRIzol™ reagent (Invitrogen™; Thermo Fisher Scientific, Inc.). The synthesis of complementary DNA (cDNA) was performed using the PrimeScript™ RT kit (cat. no. RR055A; Takara Biotechnology, Co., Ltd.). Reverse transcription was performed at 37˚C for 15 min, followed by heating at 85˚C for 5 sec. Quantitative PCR was performed using Sybr Green fluorophore (Vazyme; cat. no. Q311-02/03). The PCR protocol involved initial denaturation at 95˚C for 15 sec, followed by 40 cycles of 95˚C for 15 sec and 60˚C for 60 sec. Gene expression changes were assessed using the $2^{-\Delta\Delta Cq}$ method. The primers were synthesized by Hangzhou Qingke Biotechnology Co., Ltd. and their sequences are listed in Table SII.

Immunohistochemistry. The tissue was fixed overnight in a 4% paraformaldehyde solution at room temperature. Following fixation, the sample underwent dehydration through a series of ethanol solutions, followed by treatment with xylene for tissue transparency. Subsequently, the tissue was immersed in paraffin at 65˚C and embedded in paraffin wax. Thin sections (2.5 μm thick) were sliced from the paraffin block and mounted onto glass slides. Tissue sections mounted on glass microscope slides were deparaffinized in xylene and rehydrated in graded alcohols. Subsequently, the tissue sections were boiled for 15 min in 10 mM citric acid buffer (pH 6.0) for antigen retrieval. After the sections were cooled to room temperature, they were incubated with 3% H_2O_2 for 15 min at 37˚C to block endogenous peroxidase activity. The sections were then blocked with 5% goat serum (Scientific Phygene®; Fuzhou Phygene Biotechnology Co., Ltd.) for 45 min at room temperature, and incubated with FN1 primary antibodies (1:1,000; Abcam; cat. no. ab2413) overnight at 4˚C. Subsequently, the sections were incubated with, including goat anti-rabbit IgG secondary antibodies (1:1,000; Abcam; cat. no. ab150077) for 30 min at room temperature. Finally, the substrate color was developed using a diaminobenzidine substrate kit (Abcam; cat. no. ab64238), and the sections were counterstained with hematoxylin for 30 sec at room temperature. Images were captured using a light microscope (Nikon Corporation) and the immunohistochemistry results were quantified using ImageJ software (version 1.8.0; National Institutes of Health).

Clinical statistical analysis of prognosis and assessment of FN1 expression. The progression-free interval (PFI) of the prognostic parameters were assessed using patient data from TCGA within the clinical interpretation module of the Xiantao platform (https://www.xiantaozi.com/).The median value served as the threshold to categorize the FN1 gene expression groups into low and high categories.

Statistical analysis. In the analysis of clinical variables, age, T stage, N stage, M stage, histological type, primary neoplasm focus type, and FN1 expression were chosen for univariate Cox regression analysis. Kaplan-Meier methods were employed to assess the progression-free interval (PFI) of these prognostic factors. The association between clinical-pathological characteristics and FN1 gene expression was assessed using the Wilcoxon rank-sum test in conjunction with logistic regression. Furthermore, a multivariate Cox regression model was used to evaluate the impact of FN1 gene expression on survival probability and other clinical variables. The Wilcoxon rank-sum test was used for comparing two groups and one-way analysis of variance (ANOVA) was used to compare multiple groups, followed by Tukey's post hoc test for pairwise comparisons. Correlation analyses were performed using Spearman's rank correlation coefficient and distance correlation methodologies. Fisher's exact test or the χ^2 test were used to assess statistical significance for categorical variables between two groups. Statistical P-values were two-sided, with $P<0.05$ considered to indicate a statistically significant difference. Data processing was performed using R software, (version 4.2.0; https://www.r-project.org/).

Results

Genomic differences between normal thyroid and THCA tissues. Based on 337 normal samples and 509 tumor samples from the TCGA and GTEx datasets, systematic clustering demonstrated the genomic differences between the normal tissues and THCA tissues (Fig. 1A). Principal component

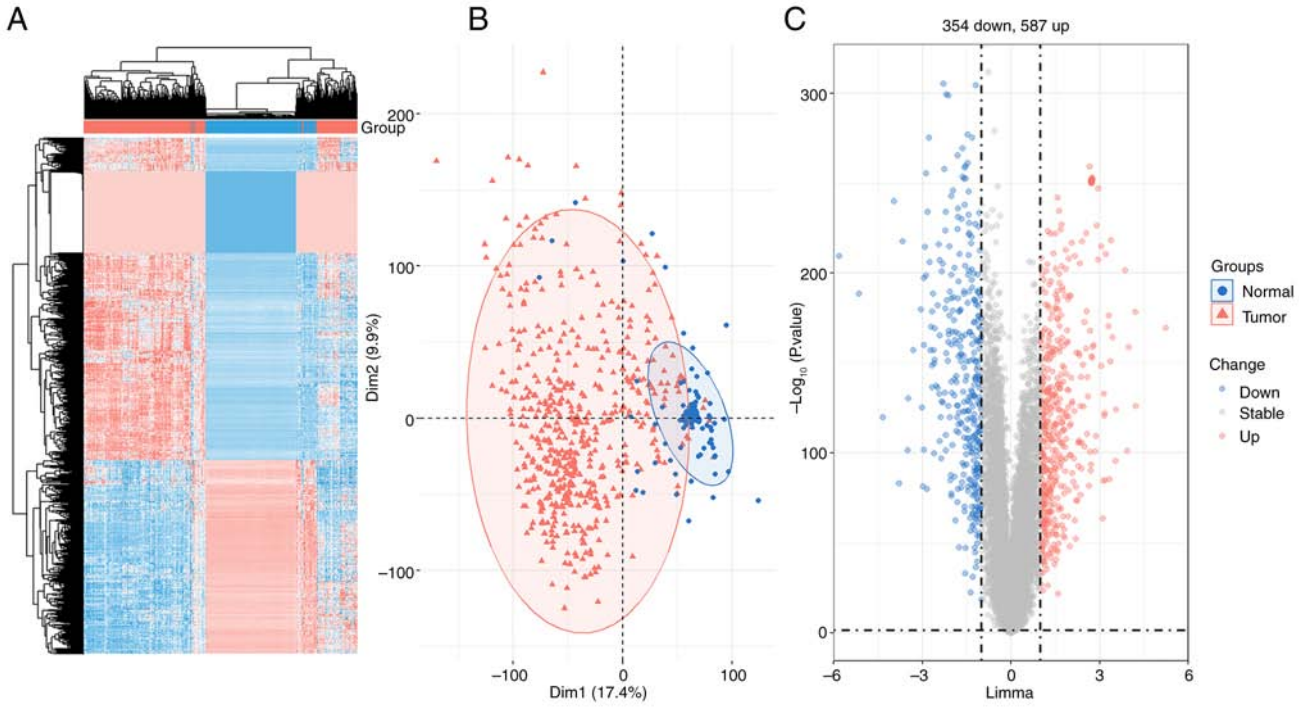

Figure 1. Differentially expressed genes in the normal and THCA groups. (A) Heatmap depicting prominently upregulated (red) and downregulated (blue) genes in normal and THCA groups, based on the cutoff criteria of log2 (fold change) >1 and P<0.05. (B) Principal Component Analysis of the THCA (red) and matched normal (blue) groups. (C) Volcano plot illustrating prominently upregulated (red) and downregulated (blue) genes in the THCA and normal groups, using a cut-off threshold of log2 (fold change) >1 and P<0.05. THCA, thyroid cancer.

analysis (PCA) revealed a marked separation between the control group and the tumor group, but the similarity between the two groups was small (Fig. 1B). The volcano map of DEGs included 587 upregulated genes and 354 downregulated genes in THCA tissues compared with paired normal tissues (Fig. 1C). 941 genes in THCA samples were revealed to have significantly different expressions in comparison with normal samples (P<0.05 and logFC >1) (Fig. 1C).

Identification of THCA-related modules by WGCNA. Genes within a common functional group exhibit similar expression patterns and share expression regulation mechanisms (38). Therefore, a weighted gene co-expression network was created using the RNA-sequencing count data from the TCGA-THCA and GTEx datasets. The power of β=8 was chosen for soft-thresholding (Fig. 2A). Ultimately, 11 modules were selected using average hierarchical clustering and dynamic tree clipping methods (Fig. 2B). The correlations between the 11 modules is demonstrated in Fig. 2C. Moreover, modular trait diagrams were created to analyze the correlation between gene modules and clinical features in THCA (Fig. 2D). The two modules with the highest correlation with tumors were MEtan and MEturquoise in TCGA-THCA (Fig. 2D).

Intersection of DEGs and co-expression module genes (CEMGs). A total of 426 overlapping genes were identified between the DEGs and the top two most relevant CEMGs. These genes have been identified as candidate hub genes for THCA and were subsequently used in further analyses (Fig. 3A and Table SIII).

Enrichment analyses of the 426 overlapping genes. The BP category was enriched with GO terms that predominantly encompassed synapse organization, wound healing, epidermis development and skin development (Fig. 3B). Within the CC category, the enriched terms primarily encompassed collagen-containing ECM, endoplasmic reticulum lumen, basal part of the cell and basal plasma membrane. Furthermore, in the MF category, the enriched terms predominantly consisted of sulfur compound binding, serine-type endopeptidase activity, serine-type peptidase activity and serine hydrolase activity. Additionally, KEGG pathway analysis revealed significant enrichments in transcriptional misregulation in cancer, cell adhesion molecules and ECM-receptor interaction (Fig. 3C).

Identifying hub genes in the PPI network. A PPI network was established to assess the interconnections among the protein-encoding DEGs associated with THCA. Among these DEGs, the foremost five genes, namely FN1, mucin-1 (MUC1), keratin (KRT) 19, intracellular adhesion molecule 1 (ICAM1) and neural cell adhesion molecule (NCAM1), were identified as key molecules due to their notable connectivity (Fig. 4).

Validation of protein and gene-expression levels of THCA-related hub genes. Immunohistochemistry staining outcomes for five key genes were derived from the Human Protein Atlas (HPA) database (https://www.proteinatlas.org/). In comparison with the normal group, the protein expression levels of FN1, MUC1, KRT19 and ICAM1 were markedly augmented in the tumor group. Conversely, the expression of NCAM1 was notably downregulated in the tumor samples (Fig. 5). These findings highlight

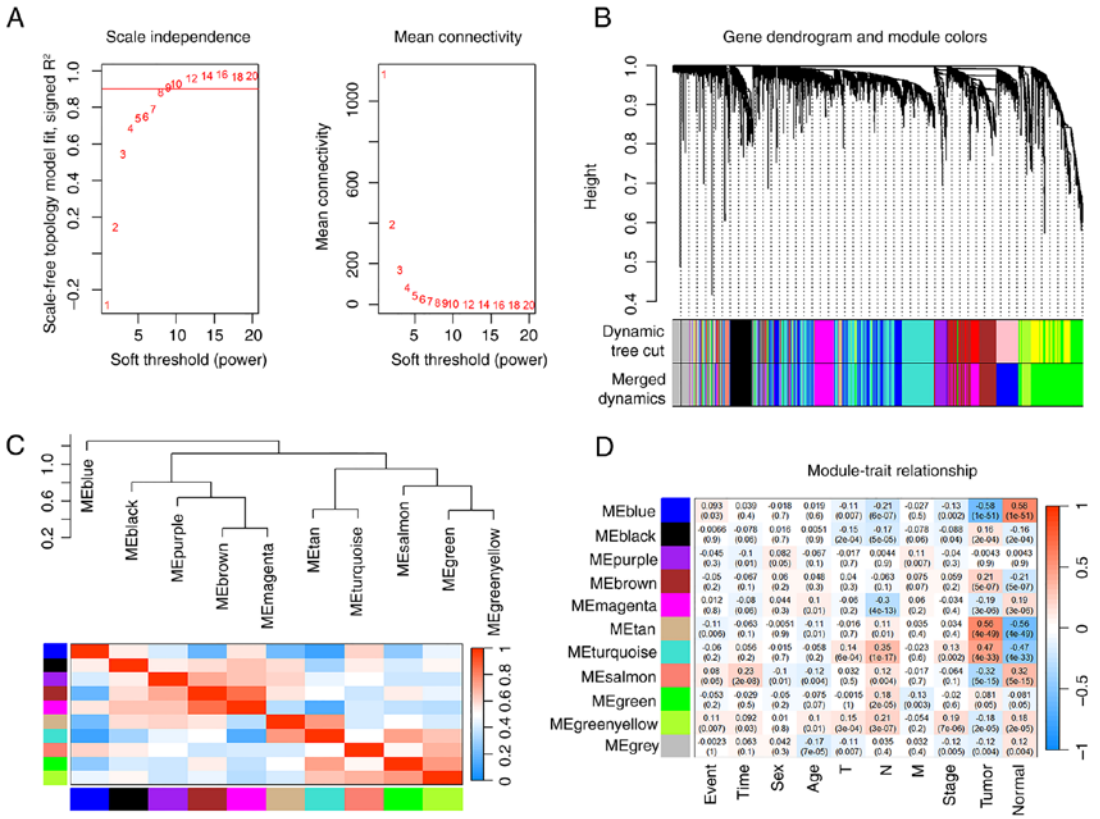

Figure 2. Modules associated with the clinical phenotype of thyroid cancer. (A) Assessment of scale independence and mean connectivity across different soft threshold powers. (B) Gene clustering using the dynamic tree cut and merged dynamic methods across multiple modules. Each branch corresponds to an individual gene, and each color signifies a distinct co-expression module. (C) Visual representation of inter-module correlation using a heatmap. (D) Correlation between clinical phenotype and weighted gene co-expression network analysis modules. The intensity of the cell color reflects the strength of the correlation. The value in parentheses denotes the P-value for the test. T, tumor; N, node; M, metastasis.

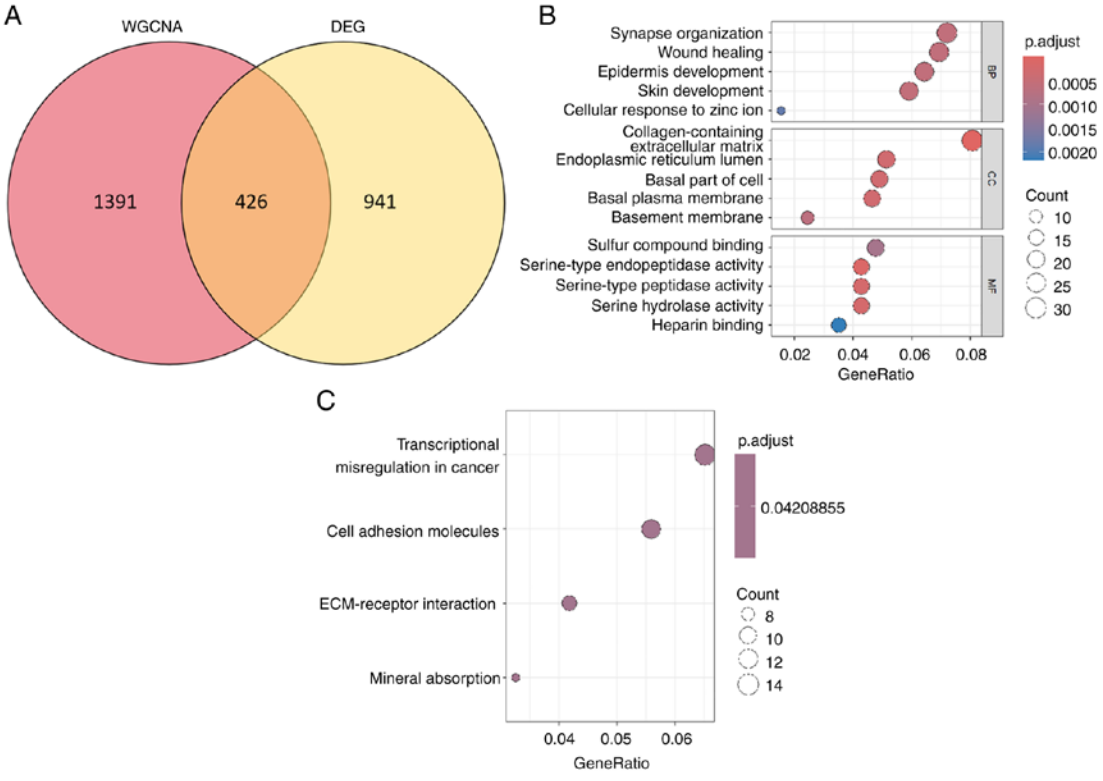

Figure 3. Functional and pathway enrichment analyses of 426 overlapping genes, visualized in a bubble plot. (A) Venn diagram of the DEGs and the top two most relevant CEMGs of thyroid cancer. (B) Gene Ontology term enrichment analyses. (C) Kyoto Encyclopedia of Genes and Genomes pathway enrichment analyses. DEG, differentially expressed genes; WGCNA, weighted gene co-expression network analysis; CEMG, co-expression module gene.

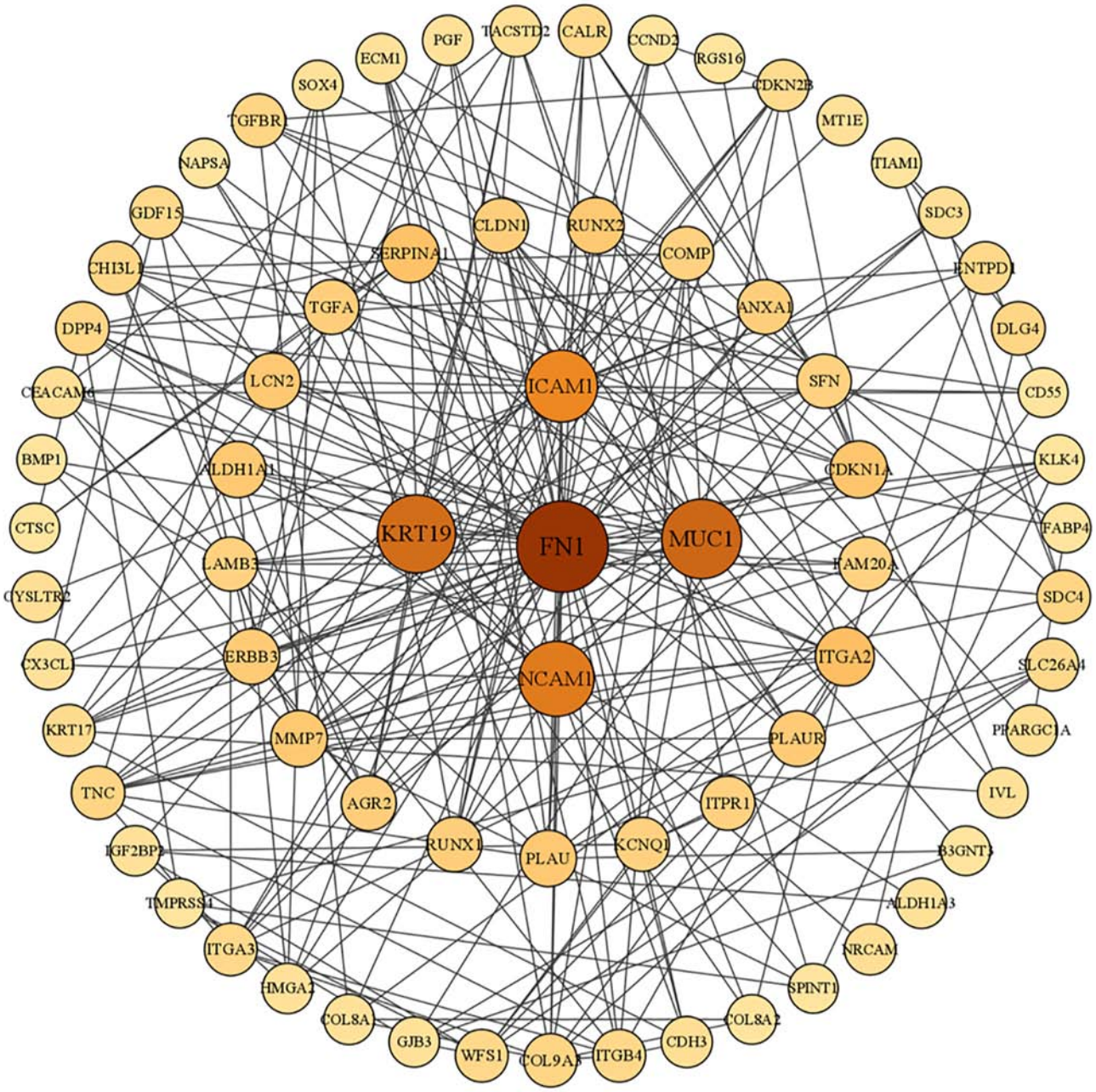

Figure 4. Top five significant hub genes identified within the protein-protein interaction networks.

the differences in the expression of selected target genes between normal and tumor tissues. Furthermore, the expression of these key molecules within THCA tissues was significantly increased compared with that in normal tissues (Fig. 6A and B). Furthermore, Spearman's correlation analyses revealed significant positive correlations between these key molecules (Fig. 6C and D). The mRNA expression levels of the five genes in the external validation datasets (GSE33630 and GSE54958) also demonstrated similar findings to those in TCGA (Fig. 6E and F). Moreover, to assess the mRNA expression variations of key molecules between normal and THCA tissues in patients, FN1, ICAM1, KRT19, MUC1, and NCAM1 levels were assessed using RT-qPCR. The results revealed that, compared with in normal tissues, the mRNA expression levels of FN1, ICAM1, KRT19 and MUC1 were significantly increased, whilst NCAM1 expression was significantly decreased, in THCA tissues (Fig. 6G).

Evaluation of TME immune cell infiltration characterization. To assess of the roles of the identified key molecules in TME immune cell infiltration, correlation analyses were performed between key genes, TME-infiltrating cells and immune checkpoint inhibitors. Using the PCA algorithm, unique enrichments of immune cell populations were revealed within the two groups (Fig. 7A). FN1, MUC1, KRT19 and ICAM1 were significantly correlated with an upregulation of immune checkpoint proteins including, PD-L1, PD-L2 and cytotoxic T-lymphocyte associated protein 4. These findings indicate significant upregulation of most immune checkpoint proteins in the tumor group, suggesting a potential association between THCA and a suppressive TME (Fig. 7B). Similarly, the results

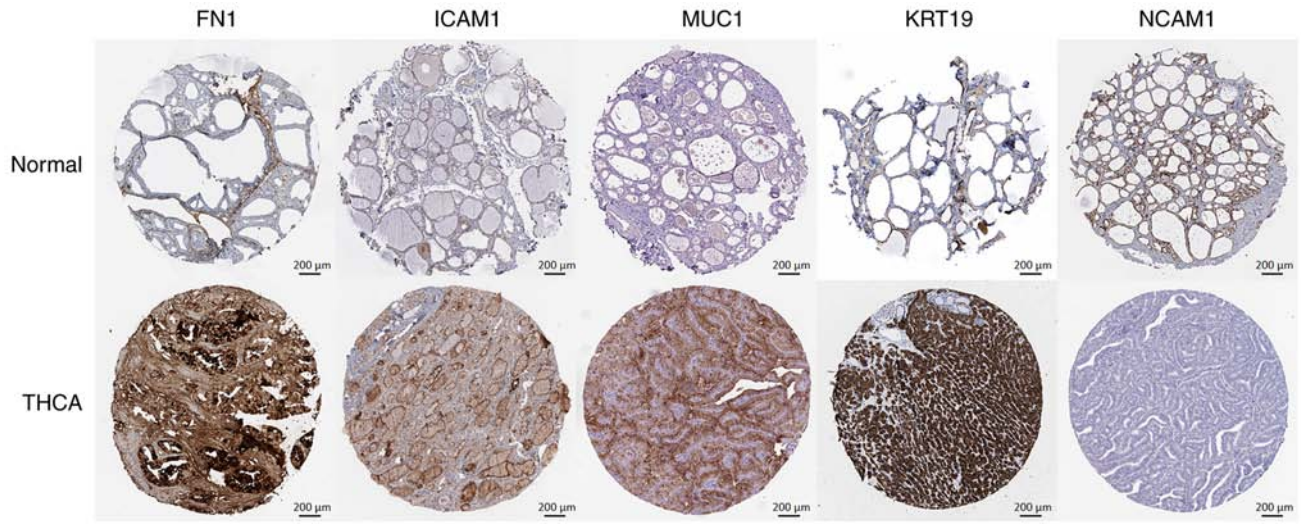

Figure 5. Immunohistochemical images of five hub genes in cancer and normal tissues from the Human Protein Atlas database. THCA, thyroid cancer; FN1, fibronectin 1; ICAM1, intracellular adhesion molecule 1; MUC1, mucin-1; KRT16, keratin 19; NCAM1, neural cell adhesion molecule.

demonstrated a significant correlation with a decrease in FN1, MUC1, KRT19 and ICAM1 within immune infiltration in monocytes, activated B cells and eosinophils, with a notable increase in other immune cell subtypes too. In contrast, NCAM1 demonstrated an inverse pattern (Fig. 7C).

Association of FN1 expression with clinical parameters and the prognostic relevance of FN1 expression. A higher tumor (T) stage, node (N) stage, pathological stage, extrathyroidal extension and PFI event was significantly associated with increased levels of FN1 expression (Fig. 8A-E). Similarly, increased FN1 expression was significantly associated with an unfavorable (PFI) outcome (Fig. 8F). Comparable results were obtained using Fisher's exact test or the χ^2 test (Table I). Moreover, the univariate analysis of FN1 expression revealed a significant association between FN1 expression and clinical parameters, specifically T stage, N stage, pathological stage and histological type (Table II). These findings demonstrate a relationship between FN1 expression, clinical characteristics and the prognosis of patients with THCA.

GSEA of the FN1 gene expression. Using TCGA gene expression data, GSEA was performed to determine the biological and functional pathways between high- and low-FN1 gene expression groups. Based on the normalized enrichment scores, the enrichment signaling pathway that was determined to be the most relevant for FN1 gene expression was chosen (Fig. 9). The GSEA analysis revealed that the high FN1 gene expression phenotype was significantly and predominantly concentrated in the Jak Stat signaling pathway, autoimmune thyroid disease, focal adhesion, disease of the immune system, cell cycle, apoptosis, cell migration and invasion, and ECM receptor interaction. The findings indicate that FN1 likely serves a significant role in the progression of THCA.

Experimental assessment of FN1 protein expression. FN1 serves a crucial role in cell adhesion and migration processes across several biological events, including embryo development, wound healing, blood clotting, host defense, metastasis and cell proliferation (39). To assess the variations in the mRNA and protein expression of FN1 between paracancerous tissue and THCA tissues, the expression levels of THCA was evaluated in tissues using immunohistochemistry. A total of four types of THCA were assessed and the resulted and demonstrated that FN1 expression levels were significantly higher in THCA tissues compared with their adjacent counterparts (Fig. 10A and B).

FN1 prognostic significance. Patients with papillary carcinoma and follicular carcinoma were excluded due to their favorable prognosis. The prognostic value of FN1 was evaluated using Kaplan-Meier survival analysis. Patients diagnosed with THCA with low FN1 expression levels demonstrated a significant survival advantage compared with those with high FN1 expression levels (Fig. 10C). This suggests that FN1 has potential prognostic significance in THCA, and may serve as a therapeutic target for THCA treatment.

Discussion

The current standard approach for comprehensive treatment of THCA involves a multifaceted strategy that combines surgery, thyroid hormone therapy and internal radiotherapy (40). However, the poor prognosis of THCA can be attributed to several factors, such as advanced clinical stage upon diagnosis and the limited availability of molecular biomarkers. Thus, there is an urgent need to identify new prognostic biomarkers and therapeutic targets in the field of cancer research.

The present study demonstrated that FN1 was highly expressed in THCA, with a logFC value of 4.22 and $P<0.001$. Previous studies have highlighted the notable role of epithelial-mesenchymal transition (EMT) in regulating THCA cell invasion and metastasis (41,42). FN1 is recognized as a biomarker for EMT and serves a crucial role in cell adhesion and migration (43). Additionally, research suggests an association between immune cell infiltration, immune markers and FN1 expression in THCA, indicating the potential role of FN1 in tumor immunology and its potential usefulness as a cancer

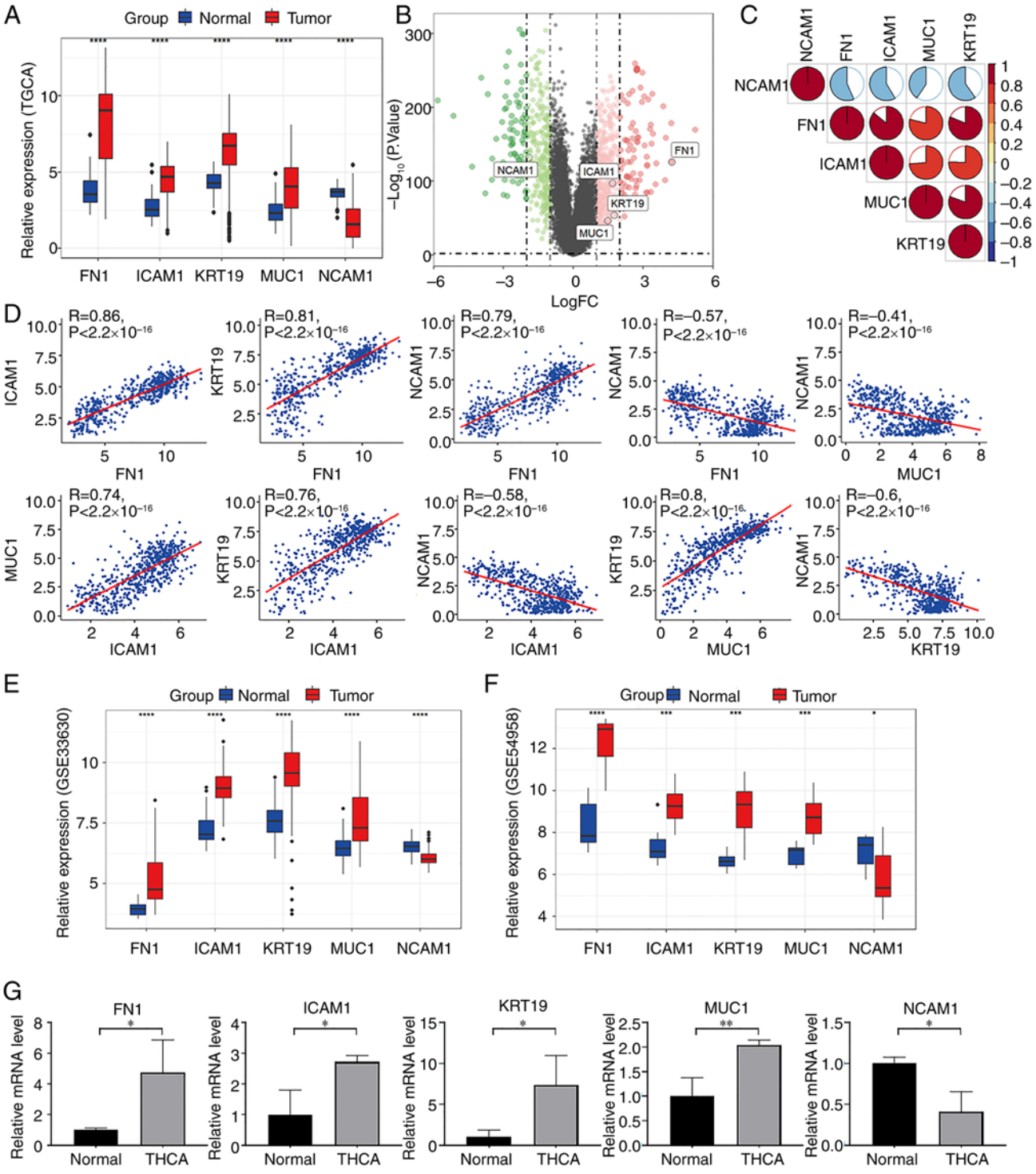

Figure 6. Identification of pivotal molecules in THCA. (A) Gene expression patterns of the target genes in THCA. (B) Volcano plot of significantly upregulated (red) and downregulated (green) genes. (C) The mRNA expression levels of FN1, ICAM1, KRT19, MUC1 and NCAM1 were found to be correlated. (D) The mRNA expression levels of FN1, ICAM1, KRT19 and MUC1 were positively correlated. By contrast, NCAM1 was negatively correlated with them. (E) The mRNA expression levels of FN1, ICAM1, KRT19 and MUC1 were notably higher in THCA tissues than in normal tissues in dataset GSE33630. Conversely, NCAM1 showed reduced expression. (F) The mRNA expression levels of FN1, ICAM1, KRT19 and MUC1 were significantly elevated in THCA tissues compared with normal tissues in dataset GSE54958. By contrast, NCAM1 exhibited decreased expression. (G) Expression levels of key molecules detected by reverse transcription-quantitative PCR. *P<0.05; **P<0.01; ***P<0.001; ****P<0.0001. THCA, thyroid cancer; FN1, fibronectin 1; ICAM1, intracellular adhesion molecule 1; MUC1, mucin-1; KRT16, keratin 19; NCAM1, neural cell adhesion molecule; TCGA, The Cancer Genome Atlas; FC, fold change;

biomarker (44). In recent years, numerous studies have highlighted the role of FN1 in tumor immune regulation (45-47). However, a comprehensive understanding of its role in the development of THCA remains elusive. In the present study, FN1 was identified as a potent biomarker for predicting the prognosis of THCA, closely associated with immune cell infiltration in solid tumors. These findings offer novel insights into the potential role of FN1 in THCA for further investigation.

Furthermore, the present study assessed the expression of FN1 and its significantly associated gene transcription data

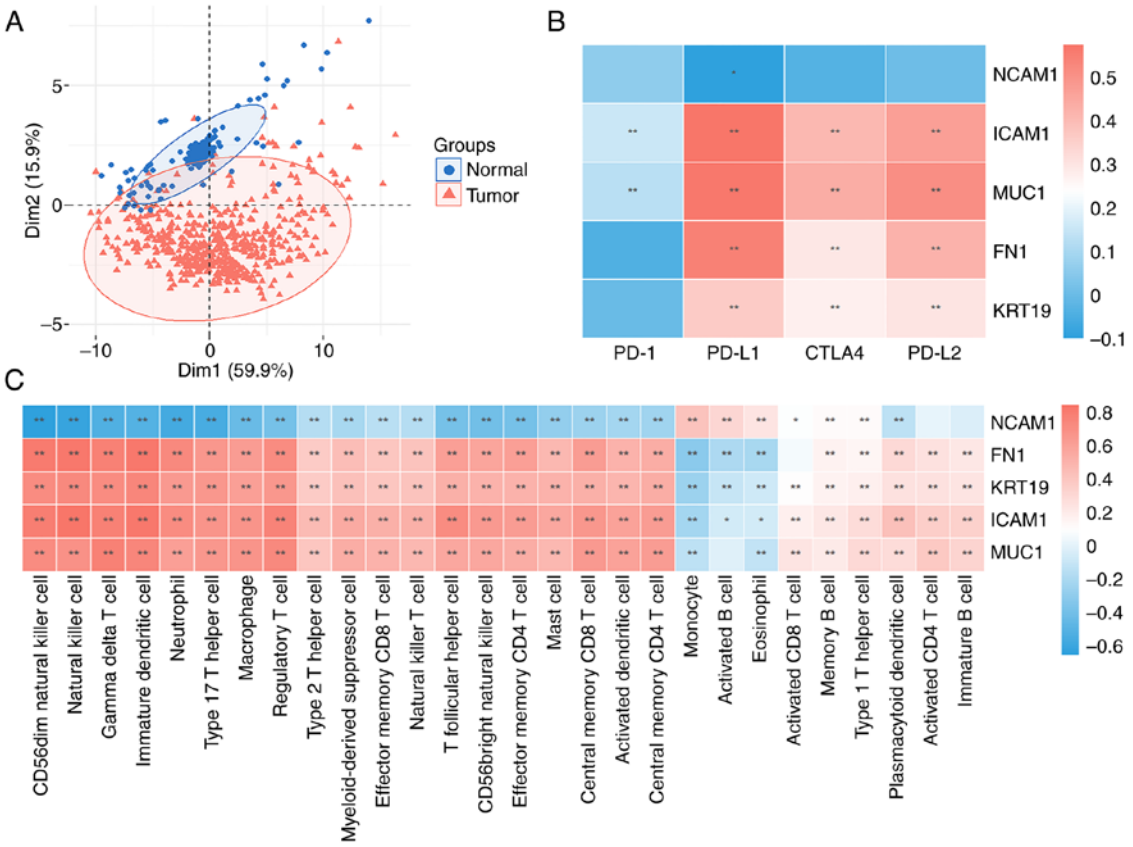

Figure 7. Evaluation of immune cell infiltration characterization. (A) Principal Component Analysis of the 28 TME infiltration cells. Association between each key gene and individual (B) TME infiltration cell types and (C) immune checkpoint inhibitors. *P<0.05; **P<0.01. TME, tumor microenvironment; PD-1, programmed cell death protein 1; PD-L, programmed death-ligand; CTLA4, cytotoxic T-lymphocyte associated protein 4; FN1, fibronectin 1; ICAM1, intracellular adhesion molecule 1; MUC1, mucin-1; KRT16, keratin 19; NCAM1, neural cell adhesion molecule.

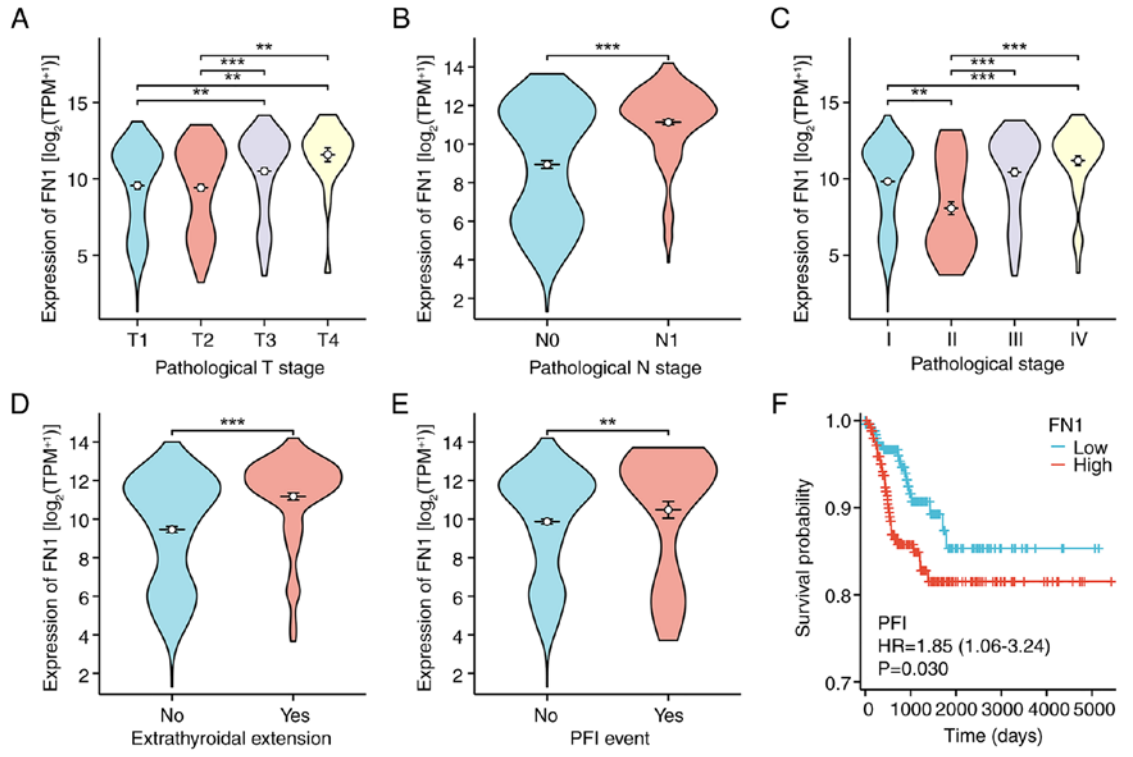

Figure 8. Association between FN1 expression and the clinical-pathological parameters of thyroid cancer, and FN1 expression prognostic analysis. Association between FN1 expression and (A) T stage, (B) N stage, (C) pathological stage, (D) extrathyroidal extension and (E) PFI event. (F) Patients with high FN1 expression had unfavorable prognosis indicators. **P<0.01; ***P<0.001. ns, no statistical difference; FN1, fibronectin 1; T, tumor; N, node; PFI, progression-free interval; TPM, transcripts per million; HR, hazard ratio.

Table I. Association between fibronectin 1 expression with clinicopathological characteristics in patients with thyroid cancer.

Characteristic	Low FN1 expression (n=256)	High FN1 expression (n=256)	P-value
Pathologic T stage			<0.001[a]
T1	81 (15.9)	62 (12.2)	
T2	99 (19.4)	70 (13.7)	
T3	67 (13.1)	108 (21.2)	
T4	8 (1.6)	15 (2.9)	
Pathologic N stage			<0.001[a]
N0	146 (31.6)	83 (18.0)	
N1	79 (17.1)	154 (33.3)	
Pathologic M stage			0.324[b]
M0	128 (43.4)	158 (53.6)	
M1	6 (2.0)	3 (1.0)	
Pathologic stage			<0.001[a]
I	151 (29.6)	137 (26.9)	
II	39 (7.6)	13 (2.5)	
III	46 (9.1)	67 (13.1)	
IV	19 (3.7)	38 (7.5)	
OS event			0.611[a]
Alive	249 (48.6)	247 (48.2)	
Dead	7 (1.4)	9 (1.8)	
Age			0.929[a]
≤45 years	121 (23.6)	122 (23.8)	
>45 years	135 (26.4)	134 (26.2)	

Data are presented as n (%). [a]χ^2 test; [b]Fisher's exact test. FN1, fibronectin 1; T, T stage; N, N stage; M, M stage; OS, overall survival.

Table II. Logistic regression analysis of fibronectin 1 expression.

Characteristic	Total (n)	OR (95% CI)	P-value
Pathological T stage (T3 and T4 vs. T1 and T2)	510	2.236 (1.553-3.220)	<0.001
Pathological N stage (N1 vs. N0)	462	3.429 (2.340-5.026)	<0.001
Pathological M stage (M1 vs. M0)	295	0.405 (0.099-1.651)	0.208
Pathological stage (Stage III and IV vs. stage I and II)	510	2.046 (1.405-2.981)	<0.001
Age (>45 years vs. ≤45 years)	512	0.984 (0.696-1.393)	0.929
Histological type (Other and tall cell vs. classical and follicular)	512	4.491 (2.116-9.533)	<0.001
Primary neoplasm focus type (Unifocal vs. multifocal)	502	1.153 (0.811-1.637)	0.428

T, T stage; N, N stage; M, M stage; OR, odds ratio; CI, confidence interval.

in thyroid tumors. The expression of FN1 in both paired and unpaired THCA samples revealed substantial upregulation. Furthermore, as proteins serve as the ultimate functional units in biology, immunohistochemical analysis was performed. In several types of THCA, FN1 expression was notably higher than in normal thyroid tissues, with expression observed in both the nucleus and cytoplasm. Immunohistochemical results from the HPA database further corroborated the reliability of the obtained data.

The present study also evaluated the clinical significance of FN1 in a cohort of patients with THCA, assessed the relationship between FN1 protein levels and clinicopathological characteristics, and confirmed the clinical utility of FN1. Analysis of clinical data demonstrated a significant correlation between FN1 expression levels and the T-stage of patients with THCA. Patients at advanced T-stages exhibited progressively elevated FN1 expression, aligning with findings in gastric cancer progression (48). Patients with medullary and undifferentiated carcinoma who exhibited low FN1 expression had prolonged survival compared with individuals with high expression levels. Consistent with previous findings in gastric cancer, breast cancer and skull base chordoma, these results

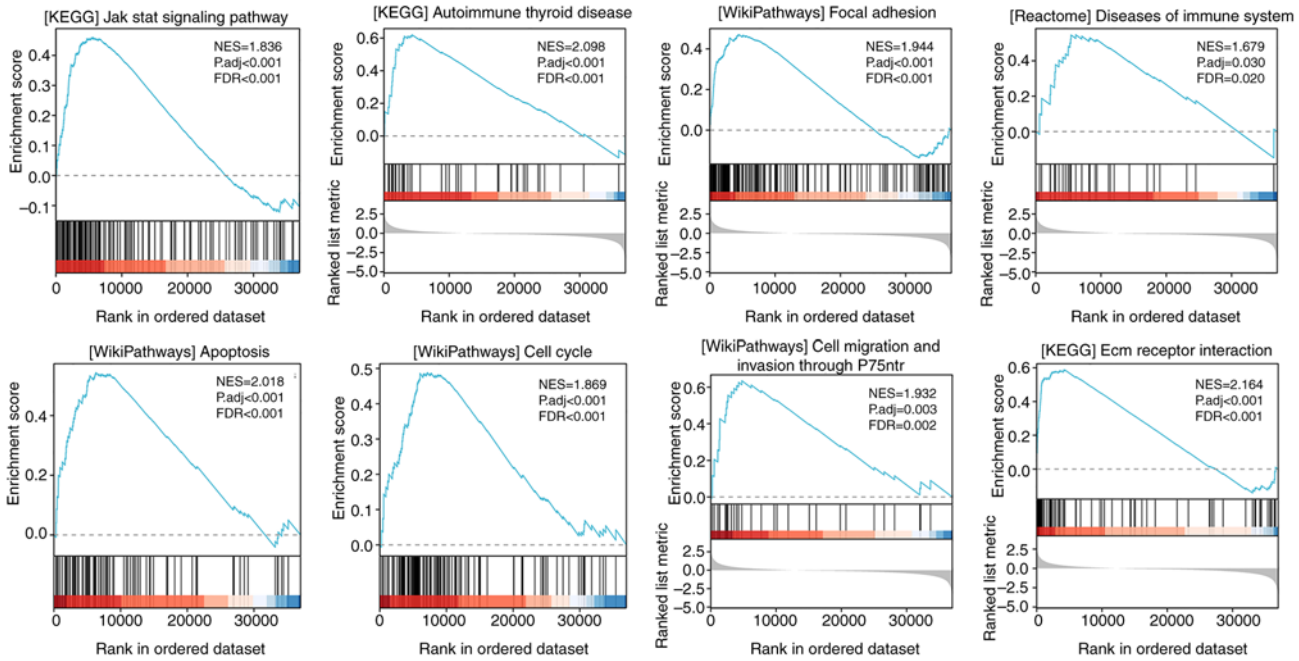

Figure 9. Findings of the Gene Set Enrichment Analysis. NES, normalized enrichment score; FDR, false discovery rate; KEGG, Kyoto Encyclopedia of Genes and Genomes.

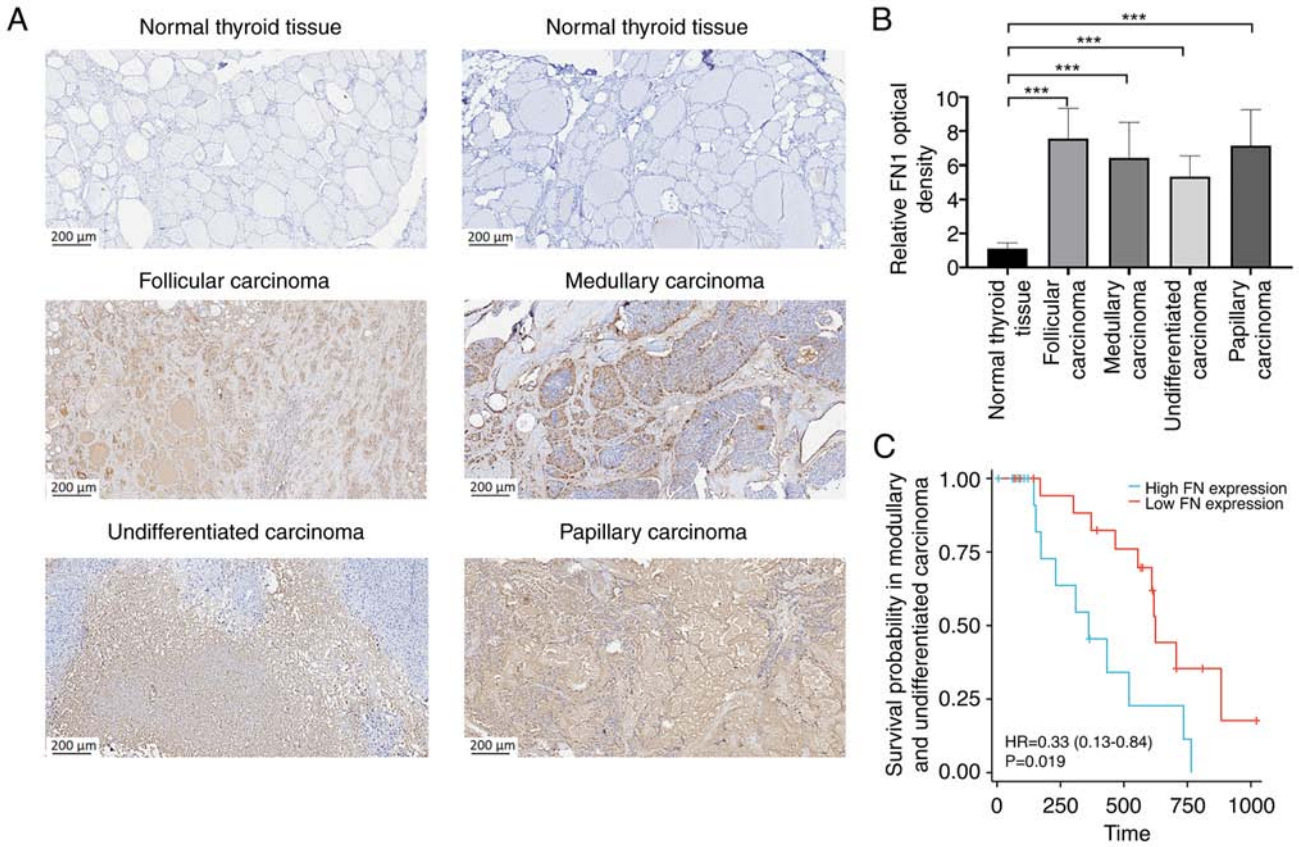

Figure 10. Levels of FN1 protein expression in patients with THCA. (A) Representative images of FN1 staining in 4 types of THCA. (B) Relative FN1 optical density. (C) Kaplan-Meier plot of the survival outcomes of patients with THCA, categorized by high (blue) or low (red) FN1 expression levels. ***P<0.001. THCA, thyroid cancer; FN1, fibronectin 1; HR, hazard ratio.

collectively suggest the involvement of FN1 as an oncogene in the progression of malignant tumors, leading to a worse prognosis (45,48,49). This indicates that FN1 can serve as an independent prognostic indicator for overall survival. Therefore, the present study provides valuable insights and practical implications by proposing FN1 as a promising

molecular marker for THCA, thus improving the clinical management of patients with THCA in the future.

Moreover, the present study explored genes that are significantly associated with FN1 expression in THCA. The findings revealed abnormal expression of these genes, indicating their direct or indirect involvement in a regulatory network with FN1, influencing the onset and progression of THCA. The present study used integrated bioinformatics methods, specifically WGCNA and DEG analysis, to identify a comprehensive set of 426 candidate hub genes that exhibited overlapping characteristics. By constructing a PPI network and applying rigorous analysis techniques, the top five hub genes were successfully pinpointed: FN1, MUC1, KRT19, ICAM1 and NCAM1. The interaction between MUC1 and adhesion molecules enables cancer cells to exploit advantageous mechanisms for invasion and metastasis (50,51). Therefore, MUC1 serves a pivotal role in maintaining epithelial cell homeostasis as well as driving cancer progression. KRTs are integral components of the cellular framework, engaging in interactions with several cellular proteins such as kinases, receptors, adaptors and effectors (52,53). These interactions initiate signaling networks that govern crucial cellular processes, including cell migration, invasion, metastasis, cell cycle progression and apoptosis. ICAM1 is actively involved in the immune process and inflammatory response within the body (54). Additionally, it serves a crucial role in mediating the adhesion of tumor cells to other cell types and the ECM by binding with specific ligands. This mechanism allows tumor cells to evade immune surveillance, facilitating their invasion and metastasis. Sasca *et al* (55) reported that the inhibition of MEK1/2 enhances the susceptibility of acute myeloid leukemia (AML) blasts to genotoxic agents, suggesting that NCAM1 can serve as a useful biomarker for guiding AML treatment. These findings indicate that the activation of FN1 may be closely associated with immune evasion, invasion and metastasis, and collectively endow tumor cells with the ability to resist harsh environmental conditions.

GSEA was also performed to enhance comprehension of FN1 function and its associated activation pathways. The GSEA analysis revealed the involvement of FN1 in regulating the malignant phenotype of THCA, as well as its participation in pathways linked with cell adhesion molecules, tight junctions and ECM-receptor interactions associated with the migratory and invasive functions of tumor cells. Notably, FN1 extensively influences immune-related pathways, suggesting its role as an oncogene in modulating the immune microenvironment of tumors. Based on these pivotal findings, the correlation between FN1 and immune-infiltrating cells was subsequently assessed. FN1 was demonstrated to significantly impact immune cell infiltration within solid tumors, with the high-expression group of FN1 showing marked increases in NK, CD4T and CD8T cells compared with the low-expression group. NK cells, being innate immune cells, possess the ability to directly recognize tissues expressing major histocompatibility complex class I molecules and eliminate foreign or stressed target cells, including those affected by viral infections, aging or cancer transformations (56). These findings suggest that FN1 plays a pivotal regulatory role in malignant solid tumors, promoting tumor progression. Additionally, FN1 shows widespread expression in immune cells within the tumor microenvironment (TME).

However, whilst the present study has identified FN1 as a promising therapeutic target for THCA, involved in immune microenvironment regulation and closely linked with prognosis, it is not without limitations. Firstly, the precise mechanism through which FN1 modulates immune cells in the TME necessitates validation through a series of meticulously designed experiments. Moreover, the use of FN1 as a prognostic marker for THCA requires confirmation in clinical applications from bench to bedside. Nevertheless, the findings of the present study emphasize future research directions aimed at providing potential insights into the development of new treatment modalities for THCA.

In conclusion, FN1 is upregulated in advanced THCA, which may affect THCA progression via key molecular functions and pathways. The acquired data suggest that FN1 is a powerful and promising biomarker for predicting THCA prognosis.

Acknowledgements

Not applicable.

Funding

The present work was supported by Zhejiang Provincial Medical and Health Science and Technology Project (grant no. 2024KY1089).

Availability of data and materials

The data generated in the present study may be requested from the corresponding author.

Authors' contributions

HP, ZL and FL undertook the research, analyzed the data and wrote the paper. JZ, TX and YH helped to analyzed the data. YY and BS designed the research and revised the paper. YY and BS confirm the authenticity of all the raw data. All authors have read and approved the final manuscript.

Ethics approval and consent to participate

Ethical approval for the study was granted by the Clinical Research Ethics Committee of The Second Affiliated Hospital, Zhejiang University School of Medicine (Hangzhou, China; approval nos. 2024-0005 and 2020-0559). Informed consent was waived by the Ethics Committee. All methods were performed in accordance with relevant guidelines and regulations.

Patient consent for publication

Not applicable.

Competing interests

The authors declare that they have no competing interests.

References

1. Zhou YL, Zheng C, Chen YT and Chen XM: Underexpression of INPPL1 is associated with aggressive clinicopathologic characteristics in papillary thyroid carcinoma. Onco Targets Ther 11: 7725-7731, 2018.
2. Cabanillas ME, McFadden DG and Durante C: Thyroid cancer. Lancet 388: 2783-2795, 2016.
3. Ge J, Wang J, Wang H, Jiang X, Liao Q, Gong Q, Mo Y, Li X, Li G, Xiong W, *et al*: The BRAF V600E mutation is a predictor of the effect of radioiodine therapy in papillary thyroid cancer. J Cancer 11: 932-939, 2020.
4. Ma T, Wang R, Zhou X, Liu L, Pan A, Wang H and Huang L: Case reports of collision and composite carcinomas of the thyroid: An insight into their origin and clinical significance. BMC Endocr Disord 23: 173, 2023.
5. Wan Y, Zhang X, Leng H, Yin W, Zeng W and Zhang C: Identifying hub genes of papillary thyroid carcinoma in the TCGA and GEO database using bioinformatics analysis. PeerJ 8: e9120, 2020.
6. Ejiofor EU, Ishebe JE, Benjamin I, Okon GA, Gber TE and Louis H: Exploring the potential of single-metals (Cu, Ni, Zn) Decorated $Al_{12}N_{12}$ nanostructures as sensors for flutamide anticancer drug. Heliyon 9: e20682, 2023.
7. Feng G, Chen C and Luo Y: PRMT1 accelerates cell proliferation, migration, and tumor growth by upregulating ZEB1/H4r3me2as in thyroid carcinoma. Oncol Rep 50: 210, 2023.
8. Xu W, Wang L, An Y and Ye J: Expression of WD repeat domain 5 (WDR5) is associated with progression and reduced prognosis in papillary thyroid carcinoma. Med Sci Monit 25: 3762-3770, 2019.
9. Liu X, Huang Z, He X, Zheng X, Jia Q, Tan J, Fan Y, Lou C and Meng Z: Blood prognostic predictors of treatment response for patients with papillary thyroid cancer. Biosci Rep 40: BSR20202544, 2020.
10. Liao Z, Cheng Y, Zhang H, Jin X, Sun H, Wang Y and Yan J: A novel prognostic signature and immune microenvironment characteristics associated with disulfidptosis in papillary thyroid carcinoma based on Single-Cell RNA sequencing. Front Cell Dev Biol 11: 1308352, 2023.
11. Soll D, Bischoff P, Frisch A, Jensen M, Karadeniz Z, Mogl MT, Horst D, Penzkofer T, Spranger J, Keilholz U and Mai K: First effectiveness data of lenvatinib and pembrolizumab as First-Line therapy in advanced anaplastic thyroid cancer: A retrospective cohort study. BMC Endocr Disord 24: 25, 2024.
12. Tan JSH, Tay TKY, Ong EHW, Fehlings M, Tan DS, Sukma NB, Chen EX, Sng JH, Yip CSP, Lim KH, *et al*: Combinatorial hypofractionated radiotherapy and pembrolizumab in anaplastic thyroid cancer. Eur Thyroid J 13: e230144, 2024.
13. Oh DY, Algazi A, Capdevila J, Longo F, Miller W Jr, Chun Bing JT, Bonilla CE, Chung HC, Guren TK, Lin CC, *et al*: Efficacy and safety of pembrolizumab monotherapy in patients with advanced thyroid cancer in the phase 2 KEYNOTE-158 study. Cancer 129: 1195-1204, 2023.
14. Yi PQ, Nie FF, Fan YB, Yu WW, Hu CS, Guo XM and Fu J: Intraoperative radiotherapy for the treatment of thyroid cancer: A pilot study. Oncotarget 8: 29355-29360, 2017.
15. Lan X, Bao H, Ge X, Cao J, Fan X, Zhang Q, Liu K, Zhang X, Tan Z, Zheng C, *et al*: Genomic landscape of metastatic papillary thyroid carcinoma and novel biomarkers for predicting distant metastasis. Cancer Sci 111: 2163-2173, 2020.
16. Suzuki S, Bogdanova TI, Saenko VA, Hashimoto Y, Ito M, Iwadate M, Rogounovitch TI, Tronko MD and Yamashita S: Histopathological analysis of papillary thyroid carcinoma detected during ultrasound screening examinations in fukushima. Cancer Sci 110: 817-827, 2019.
17. Ohno K, Shibata T and Ito KI: Epidermal growth factor receptor activation confers resistance to lenvatinib in thyroid cancer cells. Cancer Sci 113: 3193-3210, 2022.
18. Yu Y and Tian X: Analysis of genes associated with prognosis of lung adenocarcinoma based on GEO and TCGA databases. Medicine (Baltimore) 99: e20183, 2020.
19. Silva JCF, Carvalho TFM, Basso MF, Deguchi M, Pereira WA, Sobrinho RR, Vidigal PMP, Brustolini OJB, Silva FF, Dal-Bianco M, *et al*: Geminivirus data warehouse: A database enriched with machine learning approaches. BMC Bioinformatics 18: 240, 2017.
20. Pankov R and Yamada KM: Fibronectin at a glance. J Cell Sci 115: 3861-3863, 2002.
21. Malik G, Knowles LM, Dhir R, Xu S, Yang S, Ruoslahti E and Pilch J: Plasma fibronectin promotes lung metastasis by contributions to fibrin clots and tumor cell invasion. Cancer Res 70: 4327-4334, 2010.
22. Xiao J, Yang W, Xu B, Zhu H, Zou J, Su C, Rong J, Wang T and Chen Z: Expression of fibronectin in esophageal squamous cell carcinoma and its role in migration. BMC Cancer 18: 976, 2018.
23. Cai X, Liu C, Zhang TN, Zhu YW, Dong X and Xue P: Down-regulation of FN1 inhibits colorectal carcinogenesis by suppressing proliferation, migration, and invasion. J Cell Biochem 119: 4717-4728, 2018.
24. Nakagawa Y, Nakayama H, Nagata M, Yoshida R, Kawahara K, Hirosue A, Tanaka T, Yuno A, Matsuoka Y, Kojima T, *et al*: Overexpression of fibronectin confers cell adhesion-mediated drug resistance (CAM-DR) against 5-FU in oral squamous cell carcinoma cells. Int J Oncol 44: 1376-1384, 2014.
25. Wang J, Deng L, Huang J, Cai R, Zhu X, Liu F, Wang Q, Zhang J and Zheng Y: High expression of fibronectin 1 suppresses apoptosis through the NF-κB pathway and is associated with migration in nasopharyngeal carcinoma. Am J Transl Res 9: 4502-4511, 2017.
26. Waalkes S, Atschekzei F, Kramer MW, Hennenlotter J, Vetter G, Becker JU, Stenzl A, Merseburger AS, Schrader AJ, Kuczyk MA and Serth J: Fibronectin 1 mRNA expression correlates with advanced disease in renal cancer. BMC Cancer 10: 503, 2010.
27. Glasner A, Levi A, Enk J, Isaacson B, Viukov S, Orlanski S, Scope A, Neuman T, Enk CD, Hanna JH, *et al*: NKp46 Receptor-Mediated Interferon-γ production by natural killer cells increases fibronectin 1 to alter tumor architecture and control metastasis. Immunity 48: 107-119.e4, 2018.
28. Chen W, Wang J, Shi J, Yang X, Yang P, Wang N, Yang S, Xie T, Yang H, Zhang M, *et al*: Longevity effect of liuwei dihuang in both caenorhabditis elegans and aged mice. Aging Dis 10: 578-591, 2019.
29. Cao J, Huang M, Guo L, Zhu L, Hou J, Zhang L, Pero A, Ng S, El Gaamouch F, Elder G, *et al*: Microrna-195 rescues Apoe4-Induced cognitive deficits and lysosomal defects in Alzheimer's disease pathogenesis. Mol Psychiatry 26: 4687-4701, 2021.
30. Wu C, Qi X, Qiu Z, Deng G and Zhong L: Low expression of KIF20A suppresses cell proliferation, promotes chemosensitivity and is associated with better prognosis in HCC. Aging (Albany NY) 13: 22148-22163, 2021.
31. Shi Y, Liu W, Yang Y, Ci Y and Shi L: Exploration of the shared molecular mechanisms between COVID-19 and neurodegenerative diseases through bioinformatic analysis. Int J Mol Sci 24: 4839, 2023.
32. Shi J, Shui D, Su S, Xiong Z and Zai W: Gene enrichment and co-expression analysis shed light on transcriptional responses to Ralstonia solanacearum in tomato. BMC Genomics 24: 159, 2023.
33. Li M, Wang K, Zhang Y, Fan M, Li A, Zhou J, Yang T, Shi P, Li D, Zhang G, *et al*: Ferroptosis-Related genes in bronchoalveolar lavage fluid serves as prognostic biomarkers for idiopathic pulmonary fibrosis. Front Med (Lausanne) 8: 693959, 2021.
34. Yi X, Wan Y, Cao W, Peng K, Li X and Liao W: Identification of four novel prognostic biomarkers and construction of two nomograms in adrenocortical carcinoma: A Multi-Omics data study via bioinformatics and machine learning methods. Front Mol Biosci 9: 878073, 2022.
35. Yu J, Zhang H, Zhang Y and Zhang X: Integrated analysis of the altered lncRNA, microRNA, and mRNA expression in HBV-Positive hepatocellular carcinoma. Life (Basel) 12: 701, 2022.
36. Zhou J, Guo H, Liu L, Feng M, Yang X and Hao S: Pyroptosis patterns of colon cancer could aid to estimate prognosis, microenvironment and immunotherapy: Evidence from Multi-Omics analysis. Aging (Albany NY) 14: 7547-7567, 2022.
37. Yin S, Li X, Xiong Z, Xie M, Jin L, Chen H, Mao C, Zhang F and Lian L: A novel ceRNA-Immunoregulatory axis based on immune cell infiltration in ulcerative colitis-associated colorectal carcinoma by integrated weighted gene co-expression network analysis. BMC Gastroenterol 22: 188, 2022.
38. Adegoke A, Ribeiro JMC, Smith RC and Karim S: Tick innate immune responses to hematophagy and Ehrlichia infection at single-cell resolution. Front Immunol 14: 1305976, 2023.

39. Shaw TI, Wagner J, Tian L, Wickman E, Poudel S, Wang J, Paul R, Koo SC, Lu M, Sheppard H, *et al*: Discovery of immunotherapy targets for pediatric solid and brain tumors by Exon-Level expression. Nat Commun 15: 3732, 2024.
40. Pan Y, Wu L, He S, Wu J, Wang T and Zang H: Identification of hub genes in thyroid carcinoma to predict prognosis by integrated bioinformatics analysis. Bioengineered 12: 2928-2940, 2021.
41. Liu T, Men Q, Su X, Chen W, Zou L, Li Q, Song M, Ouyang D, Chen Y, Li Z, *et al*: Downregulated expression of TSHR is associated with distant metastasis in thyroid cancer. Oncol Lett 14: 7506-7512, 2017.
42. Xia E, Bhandari A, Shen Y, Zhou X and Wang O: LncRNA LINc00673 induces proliferation, metastasis and Epithelial-Mesenchymal transition in thyroid carcinoma via Kruppel-Like factor 2. Int J Oncol 53: 1927-1938, 2018.
43. Zhang XX, Luo JH and Wu LQ: Fn1 overexpression is correlated with unfavorable prognosis and immune infiltrates in breast cancer. Front Genet 13: 913659, 2022.
44. Geng QS, Huang T, Li LF, Shen ZB, Xue WH and Zhao J: Over-Expression and prognostic significance of FN1, correlating with immune infiltrates in thyroid cancer. Front Med (Lausanne) 8: 812278, 2021.
45. Huo X, Ma S, Wang C, Song L, Yao B, Zhu S, Li P, Wang L, Wu Z and Wang K: Unravelling the role of immune cells and FN1 in the recurrence and therapeutic process of skull base chordoma. Clin Transl Med 13: e1429, 2023.
46. Ashok G and Ramaiah S: Fn1 and cancer-associated fibroblasts markers influence immune microenvironment in clear cell renal cell carcinoma. J Gene Med 25: e3556, 2023.
47. Zhang L, Wang Y, Song M, Chang A, Zhuo W and Zhu Y: Fibronectin 1 as a key gene in the genesis and progression of Cadmium-Related bladder cancer. Biol Trace Elem Res 201: 4349-4359, 2023.
48. Li J, Chen C, Chen B and Guo T: High FN1 expression correlates with gastric cancer progression. Pathol Res Pract 239: 154179, 2022.
49. Chen C, Ye L, Yi J, Liu T and Li Z: Correction: FN1-mediated activation of aspartate metabolism promotes the progression of Triple-Negative and luminal a breast cancer. Breast Cancer Res Treat 204: 425-427, 2024.
50. Karaulov AV, Gurina NN, Novikov DV, Fomina SG and Novikov VV: Role of Muc1 expression in tumor progression. Vestn Ross Akad Med Nauk 71: 392-396, 2016 (In Russian).
51. Schroeder JA, Adriance MC, Thompson MC, Camenisch TD and Gendler SJ: MUC1 alters beta-catenin-dependent tumor formation and promotes cellular invasion. Oncogene 22: 1324-1332, 2003.
52. Saha SK, Choi HY, Kim BW, Dayem AA, Yang GM, Kim KS, Yin YF and Cho SG: KRT19 directly interacts with β-catenin/RAC1 complex to regulate NUMB-dependent NOTCH signaling pathway and breast cancer properties. Oncogene 36: 332-349, 2017.
53. Yao H, Yang Z, Liu Z, Miao X, Yang L, Li D, Zou Q and Yuan Y: Glypican-3 and KRT19 are markers associating with metastasis and poor prognosis of pancreatic ductal adenocarcinoma. Cancer Biomark 17: 397-404, 2016.
54. Yi J, Tian M, Hu L, Kang N, Ma W, Zhi J, Zheng X, Ruan X and Gao M: The mechanisms of celastrol in treating papillary thyroid carcinoma based on network pharmacology and experiment verification. Ann Transl Med 9: 866, 2021.
55. Sasca D, Szybinski J, Schüler A, Shah V, Heidelberger J, Haehnel PS, Dolnik A, Kriege O, Fehr EM, Gebhardt WH, *et al*: NCAM1 (CD56) promotes leukemogenesis and confers drug resistance in AML. Blood 133: 2305-2319, 2019.
56. Wu H, Fu Z, Li H, Fang F, He B, Ye Y, Wu H, Xu D, Zheng H and Zhang Q: TRIB3, as a robust prognostic biomarker for HNSC, is associated with poor immune infiltration and cancer cell immune evasion. Front Immunol 14: 1290839, 2023.